Chapter 3
The User's Role in Haptic System Design

Thorsten A. Kern, Christian Hatzfeld, and Fady Youssef

Abstract Consequently, a good mechanical design has to consider the user in his or her mechanical properties. The first part of this chapter deals with the discussion of the user as a mechanical *load* on the haptic device. The corresponding model is split into two independent elements depending on the frequency range of the oscillation. Methods and measurement setups for the derivation of mechanical impedance of the user are reviewed and a thorough analysis of impedance for different grip configurations is presented. In the second part of the chapter, the user is considered as the ultimate measure of quality for a haptic system. The relation of psychophysical parameters like the absolute threshold or the JND to engineering quality measures like resolution, errors and reproducibility is described and application depending quality measures like haptic transparency are introduced.

3.1 The User as Mechanical Load

Fady Youssef and Thorsten A. Kern

3.1.1 Mapping of Frequency Ranges onto the User's Mechanical Model

The area of active haptic interaction—movements, made in a conscious and controlled way by the user—is of limited range. Sources concerning the dynamics of human movements differ as outlined in the preceding chapters. The fastest conscious

Christian Hatzfeld deceased before the publication of this book.

T. A. Kern (✉) · F. Youssef
Hamburg University of Technology, Eißendorfer Str. 38, 21073 Hamburg, Germany
e-mail: t.a.kern@tuhh.de

F. Youssef
e-mail: f.youssef@tuhh.de

C. Hatzfeld
Technische Universität Darmstadt, Darmstadt, Germany

T. A. Kern et al. (eds.), *Engineering Haptic Devices*, Springer Series on Touch and Haptic Systems, https://doi.org/10.1007/978-3-031-04536-3_3

movement performed by humans is done with their fingers. Movements for typing of up to 8 Hz can be observed.[1] As these values refer to a ten-finger interaction, they have to be modified a bit. However, as the border frequency of a movement lies above the pure number of a repetitive event, an assumption of the upper border frequency of 10 Hz for active, controlled movement covers most cases.

The major part of the spectrum of haptic perception is passive (*passive haptic interaction*, Fig. 1.9). The user does not have any active influence or feedback within this passive frequency range. In fact, the user is able to modify his properties as a mechanical load by e.g. altering the force when holding a knob. But although this change influences the higher frequency range, the change itself happens with lower dynamics within the dynamic range of active haptic interaction. A look at haptic systems addressing tactile and kinaesthetic interaction channels shows that the above modeling has slightly different impacts:

- The output values of kinaesthetic systems $\underline{F}_{\text{out}}$ (Fig. 3.1a) result in two reactions by the user. First, a spontaneous, not directly controllable movement reaction $\underline{v}_{\text{spo}}$ happens as a result of the mechanical properties of the finger tip (depending on the type of grasp, this can be also the complete interior hand and its skin elasticity). Second an additional perception of forces takes place. This perception K[2] is weighted according to the actual situation and results in a conscious reaction of the motor parts of the body. These induced reactions $\underline{v}_{\text{ind}}$ summed up with the spontaneous reactions result in the combined output value $\underline{v}_{\text{out}}$ of the user.
- The movements of tactile devices $\underline{v}_{\text{out}}$ (Fig. 3.1b) and the consciously performed movement of the user $\underline{v}_{\text{ind}}$ result in a combined movement and velocity. This elongation acts on the skin, generating the output value $\underline{F}_{\text{out}}$ as a result of its mechanical properties. This conscious movement $\underline{v}_{\text{ind}}$ sums up to $\underline{v}_{\text{out}}$ in the opposite direction of the original movement, as with opposite movement directions the skin's elongation increases and results in a larger force between user and technical system. Analogously it subtracts with movements in the same direction, as in this case the device (or the user, depending on the point of view) evades the acting force trying to keep deformation low and to perceive just a small haptic feedback. According to this model only the output value $\underline{F}_{\text{out}}$ of the combined movement is perceived and contributes to a willingly induced movement.

If you transfer the model of Fig. 3.1 into an abstract notation, all blocks correspond to the transfer-function $\underline{G}_{\text{Hn}}$. Additionally, it has to be considered that the user's reaction K' is a combined reaction of complex habits and the perception K; therefore a necessity to simplify this branch of the model becomes eminent. For the purpose of device design and requirement specification, the conscious reaction is modeled by a disturbing variable only limited in bandwidth, resulting in a block-diagram according to Fig. 3.2c for kinaesthetic and according to Fig. 3.2d for tactile devices.

[1] 8 Hz corresponds to a typing speed of 480 keystrokes per minute. 400 keystrokes are regarded as very good for a professional typist, 300–200 keystrokes are good, 100 keystrokes can be achieved by most laymen.

[2] K, a variable chosen completely arbitrarily, is a helpful construct for the understanding of block-diagrams rather than having a real neurological analogy.

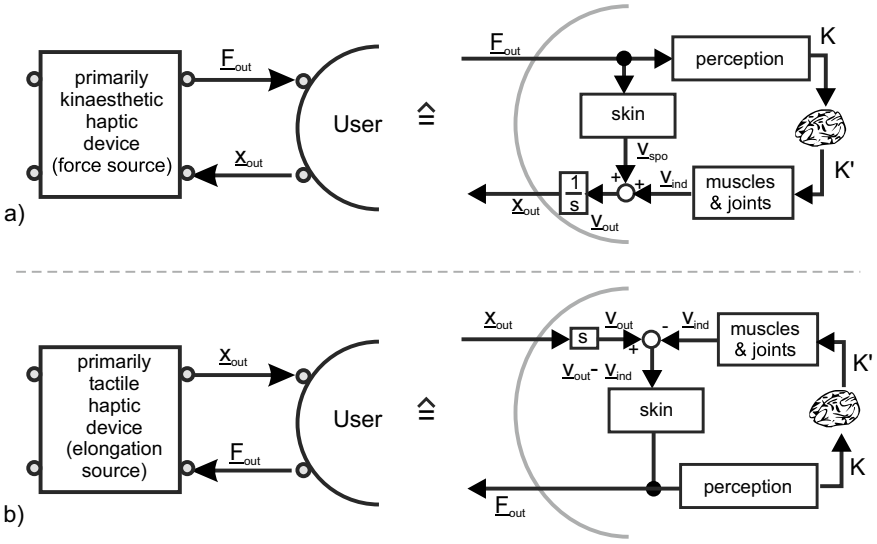

Fig. 3.1 User-models as a block-structure from kinaesthetic (a+c) and tactile (b+d) systems

The transfer function $\underline{G}_{\mathrm{H3}}$ corresponds to the mechanical admittance of the grasp above the border frequency of user interaction f_g.

With regard to the application of the presented models there are two necessary remarks to be considered:

- The notation in Figs. 3.1 and 3.2 for elongations $\underline{x}$ and forces $\underline{F}$ being input and output values of users is just one approach to the description. In fact an *impedance coupling* exists between user and haptic system making it impossible to distinguish between input and output-parameters. However, the decoupled haptic device is designed for being a position or force source. This in fact is the major motivation to define input- and/or output parameters of the user. But there are certain actuators (e.g. ultrasonic devices) which can hardly be defined as being part of either one of these classes. As a consequence, when describing either system, the choice of the leading sign and the direction of arrows should carefully be done!
- The major motivation for this model is the description of a mechanical load for the optimized dimensioning of a haptic system. For guaranteeing the closed-loop control engineering stability of a simulation or a telemanipulation system, further care has to be taken of the frequency range of active haptic interaction below 10 Hz. Stability analysis in this area can either be achieved by more detailed models or by an observation of in- and output values according to their *control-engineering passivity*. Further information on this topic can be found in Chap. 7.

The following sections on user impedance give a practical model for the transfer function $\underline{G}_{\mathrm{H3}}$ used in Fig. 3.2.

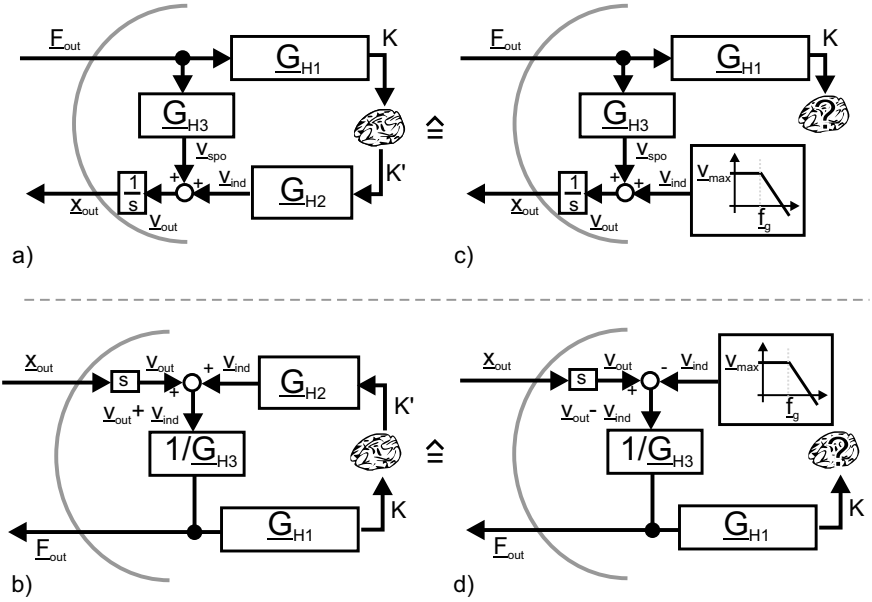

Fig. 3.2 Transformation of the user-models' block-structures in transfer-functions including simplifications of the model for the area of active haptic interaction for kinaesthetic (a+c) and tactile (b+d) systems

3.1.2 Modeling the Mechanical Impedance

The user's reaction as part of any haptic interaction combines a conscious, bandwidth-limited portion—the area of active haptic interaction—and a passive portion, mainly resulting from the mechanical properties of fingers, skin and bones. The influence of this second part stretches across the whole frequency range, but emphasizes the upper area for high frequencies. This section describes the passive part of haptic interaction. The transfer function $\underline{G}_{\mathrm{H3}}$ of Fig. 3.2 is a component of the impedance coupling with force-input and velocity-output and is therefore a mechanical admittance of the human $\underline{Y}_H$ respectively in its reciprocal value the mechanical impedance $\underline{Z}_H$.

$$\underline{G}_{\mathrm{H3}} = \frac{\underline{v}_{\mathrm{spo}}}{\underline{F}_{\mathrm{out}}} = \frac{\underline{v}_{\mathrm{out}} - \underline{v}_{\mathrm{ind}}}{\underline{F}_{\mathrm{out}}} = \underline{Y}_H = \frac{1}{\underline{Z}_H} \tag{3.1}$$

In the following, this mechanical impedance of the user will be specified. The parameter impedance combines all mechanical parameters of an object or system that can be expressed in a linear, time-invariant description, i.e. mass m, compliance k and damping d. High impedance therefore means that an object has at least one of three properties:

1. hard and stiff in the meaning of spring-stiffness
2. large mass in the sense of inertial force
3. sticky and tight in the sense of high friction

In any case a small movement (velocity $\underline{v}$) results in a high force reaction $\underline{F}$ with high impedances. Low impedance means that the object, the mechanics, is accordingly soft and light. Even high velocities result in small counter forces in this case. The human's mechanical impedance is dependent on a number of influence parameters:

- type of grasp being directly influenced by the construction of the handle
- physiological condition
- grasping force being directly influenced by the will of the user
- skin surface properties, for example skin moisture

The quantification of human's mechanical impedance requires taking as many aspects into account as possible. The type of grasp is defined by the mechanical design of the device. Nevertheless a selection of typical grasping situations will give a good overview of typical impedances appearing during human-machine interaction. The user-individual parameters like physiological condition and skin structure can be covered best by the analysis of a large number of people of different conditions. By choosing this approach a span of percentiles can be acquired covering the mechanical impedances typically appearing with human users. The "free will" itself, however, is—similar to the area of active haptic interaction—hard if not impossible to be modeled. The time dependent and unpredictable user impedance dependency on the will can only be compensated if the system is designed to cover all possible impedance couplings of actively influenced touch. Another approach would be to indirectly measure the will to adapt the impedance model of the user within the control loop. Such an indirect measure is, in many typical grasping situations, the force applied between two fingers or even the whole hand holding an object or a handle. In the simplest design the acquisition of such a force can be done by a so called *dead-man-switch*, which in 1988 was already proposed by HANNAFORD for the usage in haptic systems [11]. A dead-man-switch is pressed as long as the user holds the control handle in his or her hand. It detects the release of the handle resulting in a change in impedance from $\underline{Z}_H$ to 0.

3.1.3 Grips and Grasps

There is a nomenclature for different types of grasps shown in Fig. 3.3. The hand is an extremity with 27 bones and 33 muscles. It combines 13 (fingers) respectively 15 (incl. the wrist) degrees-of-freedom.[3] Accordingly the capabilities of man to grasp are extremely versatile.

[3] Thumb: 4 DoF, index finger: 3 DoF, middle finger: 2 DoF (sometimes 3 DoF), ring finger: 2 DoF, small finger: 2 DoF, wrist: 2 DoF. The rotation of the whole hand happens in the forearm and therefore does not count among the degrees of freedom of the hand itself.

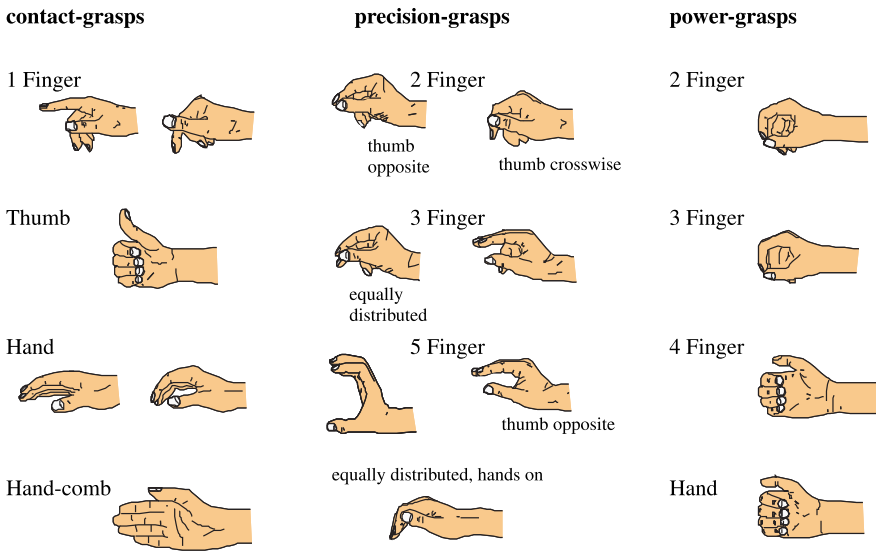

Fig. 3.3 Grip configurations, figure based on [3]

There are three classes of grasps to be distinguished:

- The **contact grasp** describes the touch of an object using the whole hand or major parts of it. Keys and buttons are typically actuated by contact grasps. Even the fingers resting on a keyboard or a piano are called contact grasps. A contact grasp always blocks one direction of movement for an object (which is one half of a degree of freedom). Contact grasps can be regarded as linear only in case of a pre-load high enough. With light touches the point of release and the according lift-off of the object is always nonlinear.
- The **precision grasp** describes the grasping with several fingers. Typically a precision grasp locks at least one degree of freedom of the grasped object by form closure with one finger and a counter bearing—often another finger. Additional degrees of freedom are hindered by friction. Precision grasps vary much in stiffness of coupling between man and machine. At the same time they are the most frequent type of grasping.
- The **power grasp** describes an object with at least one finger and a counter bearing, which may be another finger, but frequently is the whole hand. The power grasp aims at locking the grasped object in all degrees of freedom by a combination of form and force closures. Power grasps are—as the name already implies—the stiffest coupling between humans and machines.

Further discrimination of grasps is made by FEIX ET AL. and documented online [5] with the purpose of reducing the mechanical complexity of anthropomorphic hands [6]. The reported taxonomy could be useful for very specialized task-specific systems. For all classes of grasps, measurements of the human's impedance can be performed. According to the approach presented by KERN [20], the measurement

method and the models of user impedance are presented including the corresponding model parameters.

3.1.4 Measurement Setup and Equipment

The acquisition of mechanical impedances is a well-known problem in measurement technology. The principle of measurement is based on an excitation of the system to be measured by an actuator, simultaneously measuring force and velocity responses of the system. For this purpose combined force and acceleration sensors (e.g. the impedance sensor 8001 from *Brüel & Kjær*, Nærum, DK) exist, whereby the charge amplifier of the acceleration sensor includes an integrator to generate velocity signals.

In [28], WIERTLEWSKI AND HAYWARD argue that measurements with impedance heads are prone to measurement errors because of the mechanical construction of the sensor based on [2]. However, errors induced by the construction of the measurement head appear at frequencies larger than 2000 Hz, values that are only seldom used in the design of haptic interfaces. Furthermore, interpersonal variations and calibration of the measurement setup based on a concentrated network parameter approach are used to minimize the errors even for high frequencies in the following.

In general the impedance of organic systems is *nonlinear* and *time-variant*. This non-linearity is a result of a general viscoelastic behavior of tissue resulting from a combined response of relaxation, conditioning, stretching and creeping [9]. These effects can be reproduced by mechanical models with concentrated elements. However, they are dependent on the time-history of excitation to the measured object. It can be expected that measurements based on step excitation are different from those acquired with a sinusoid sweep. Additionally, the absolute time for measurement has some influence on the measures by conditioning. Both effects are systematic measurement errors. Consequently, the models resulting from such measurements are an indication of the technical design process and should always be interpreted with awareness of their variance and errors (Fig. 3.4).

All impedance measures presented here are based on a sinusoid-sweep from upper to lower frequencies. The excitation has been made with a defined force of 2 N amplitude at the sensor. The mechanical impedance of the handle has been measured by calibration measurements and was subtracted from the measured values. The impedance-sensors are limited concerning their dynamic and amplitude resolution, of course. As a consequence, the maximum frequency up to which a model is valid depends on the type of grasp and its handle used during measure. This limitation is a direct result of the amplitude resolution of the sensors and the necessity at high frequencies to have a significant difference between the user's impedance and the handle's impedance for the model to be built on. The presented model-parameters are limited to the acquired frequency range and cannot be applied to lower or higher frequencies. The measurement setup is given in Fig. 3.5.

BOCHEREAU ET AL. [1] introduced a device to record, reproduce and image the fingertip friction. In this study, Frustrated Total Internal Reflection principle (FTIR)

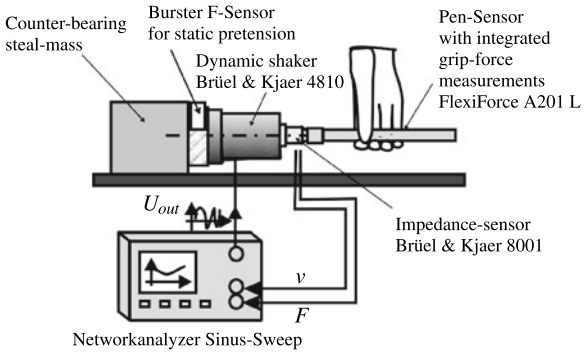

Fig. 3.4 Measurement setup for the acquisition of user impedances according to [20] © Springer Nature, all rights reserved

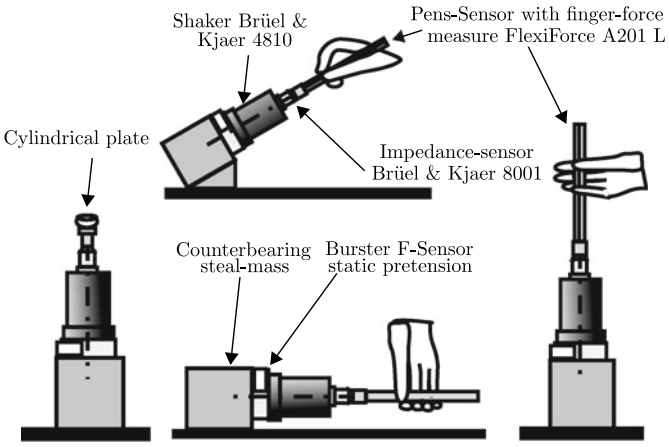

Fig. 3.5 Impedance measurement settings for different grasps

was used to image the evolution of fingertip contact area over time. The device, shown in Fig. 3.6, consists of different parts; one part is designed to record the friction force resulting from the movement of the user's finger over a texture. Three load cells are used in the record phase, in which two are used to compute the normal force and one for the tangential component. The second part of the device is designed to reproduce the friction forces, this is done with the help of a linear electrodynamic motor. The motor is connected to a glass plate, that the motor could vibrate the plate, so that the imaging phase could occur.

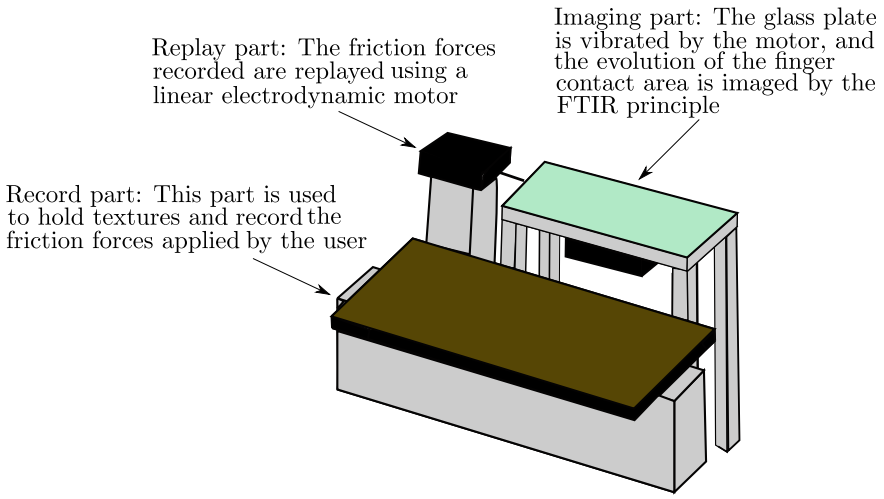

Fig. 3.6 Device to record, replay and image of finger friction movement according to [1]

3.1.5 Models

In order to approximate the human's impedance a number of different approaches were taken in the past (Fig. 3.7). For its description mechanical models based on concentrated linear elements were chosen. They range from models including active user reactions represented by force sources (Fig. 3.7a), to models with just three elements (Fig. 3.7c) and combined models of different design. The advantage of a mechanical model compared to a defined transfer function with a certain degree in enumerator and denominator results from the possibility of interpreting the elements of the model as being a picture of physical reality. Elasticities and dampers connected in circuit with the exciting force can be interpreted as the coupling to the skin. Additionally the mechanical model creates very high rankings by its interconnected elements which allow a much better fit to measurements than free transfer functions.

KERN [20] defined an eight-element model based on the models in Fig. 3.7 for the interpolation of the performed impedance measures. The model can be characterized by three impedance groups typical for many grasping situations (Fig. 3.8).

$\underline{Z}_3$ (Eq. 3.4) models the elasticity and damping of the skin being in direct contact with the handle. $\underline{Z}_1$ (Eq. 3.2) is the central element of the model and describes the mechanical properties of the dominating body parts—frequently fingers. $\underline{Z}_2$ (Eq. 3.3) gives an insight into the mechanical properties of the limbs, frequently hands, and allows to make assumptions about the pre-loads in the joints in a certain grasping situation.

$$\underline{Z}_1 = \frac{s^2 m_2 + k_1 + d_1 s}{s} \tag{3.2}$$

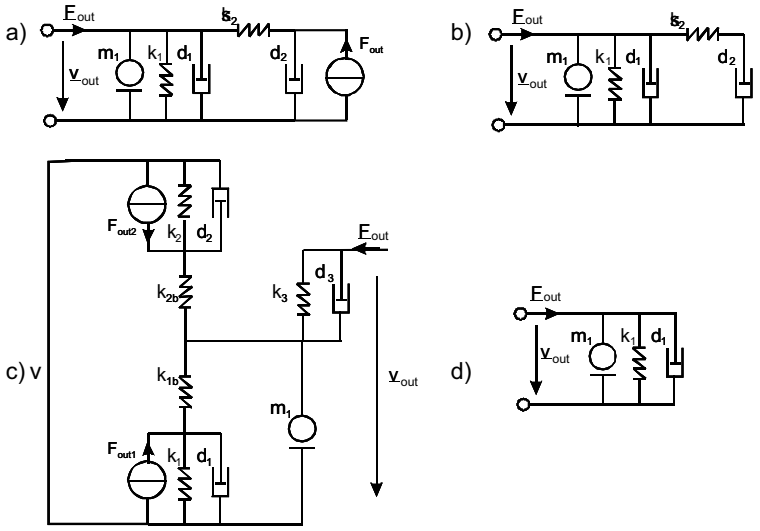

Fig. 3.7 Modeling the user with concentrated elements, **a** [11], **b** [18], **c** [23], **d** [21], own illustrations

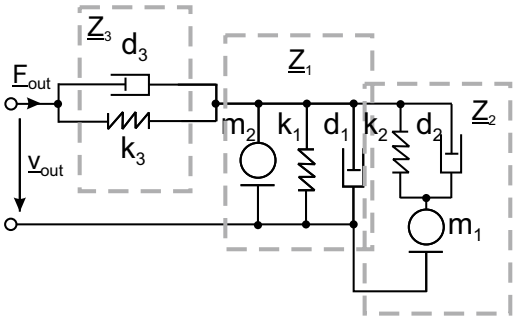

Fig. 3.8 Eight-element model of the user's impedance [20] © Springer Nature, all rights reserved, modeling the passive mechanics for frequencies >20 Hz

$$\underline{Z}_2 = \left(\frac{s}{d_2\, s + k_2} + \frac{1}{s m_1} \right)^{-1} \tag{3.3}$$

$$\underline{Z}_3 = \frac{d_3\, s + k_3}{s} \tag{3.4}$$

$$\underline{Z}_B = Z_1 + Z_2 \tag{3.5}$$

Combined, the model's transformation is given as

$$\underline{Z}_{\mathrm{H}} = \underline{Z}_3 \| \underline{Z}_B \tag{3.6}$$

$$\underline{Z}_{\mathrm{H}} = \left(\frac{s}{d_3\, s + k_3} + \left(\frac{s^2 m_2 + k_1 + d_1\, s}{s} + \left(\frac{s}{d_2\, s + k_2} + \frac{1}{s m_1} \right)^{-1} \right)^{-1} \right)^{-1} \tag{3.7}$$

3.1.6 Modeling Parameters

For above model (Eq. 3.7) the mechanical parameters can be identified by measurement and approximations with real values. For the values presented here approximately 48–194 measurements were made. The automated algorithm combines an evolutionary approximation procedure followed by a curve-fit with optimization based on NEWTON curve fitting, to achieve a final adjustment of the evolutionarily found starting parameters according to the measurement data. The measurements vary according to the mechanical pre-load—the grasping force—to hold and move the control handles. This mechanical pre-load was measured by force sensors integrated into the handles. For each measurement this pre-load could be regarded as being static and was kept by the subjects with a 5% range of the nominal value. As a result the model's parameters could be quantified not only dependent on the grasping situation but also dependent on the grasping force. The results are given in the following section. The display of the mechanical impedance is given in decibel, whereby 6 dB equals a doubling of impedance. The list of model values for each grasping situation is given in Appendix.

3.1.6.1 Precision Grasps

Within the area of precision grasps three types of grasps were analyzed. Holding a measurement cylinder similar to a normal pen in an angle of 30° (Fig. 3.9), we find a weak anti-resonance in the area of around 150–300 Hz. This anti-resonance is dependent on the grasping force and moves from weak forces and high frequencies to large forces and lower frequencies. The general dependency makes sense, as the overall system becomes stiffer (the impedance increases) and the coupling between skin and cylinder becomes more efficient resulting in more masses being moved at higher grasping forces.

The general impedance does not change significantly. if the cylinder is held in a position similar to a máobi Chinese pen (Fig. 3.10). However the dependency on the anti-resonance slightly diminishes compared to the above pen hold posture.

This is completely different to the variant of a pen in a horizontal position held by a three finger grasp (Fig. 3.11). A clear anti-resonance with frequencies between 80 and 150 Hz appears largely dependent in shape and position on the grasping force. All observable effects in precision grasps can hardly be traced back to the change of a single parameter but are always a combination of many parameters' changes.

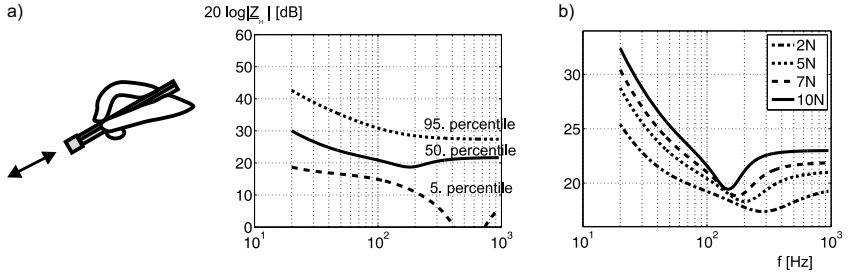

Fig. 3.9 Impedance with percentiles (**a**) and at different force levels (**b**) for a two fingered precision-grasp of a pen-like object held like a pen (Ø10 mm, defined for 20–950 Hz)

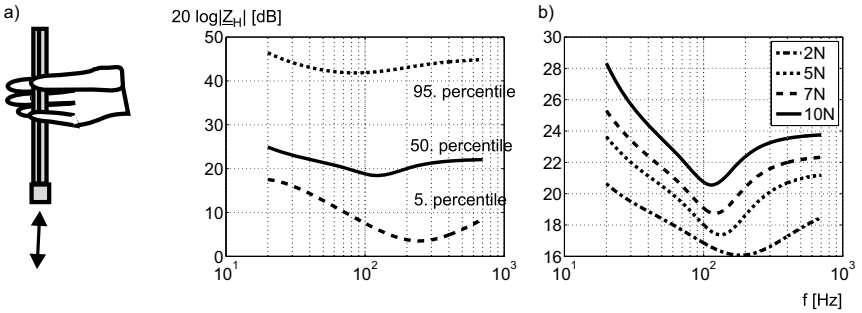

Fig. 3.10 Impedance with percentiles (**a**) and at different force levels (**b**) for a two fingered precision-grasp of a pen-like object held like a "máobi" Chinese pen (Ø10 mm, defined for 20–700 Hz)

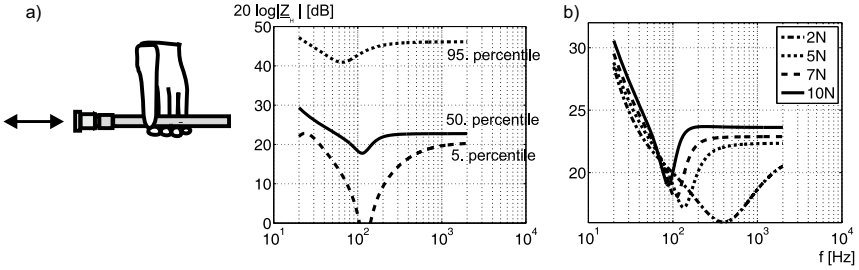

Fig. 3.11 Impedance with percentiles (**a**) and at different force levels (**b**) for a five fingered precision-grasp of a pen-like object in horizontal position (Ø10 mm, defined for 20–2 kHz)

3.1.6.2 One-Finger Contact Grasp

All measurements were done on the index finger. Direction of touch, size of touched object and touch-force normal to the skin were varied within this analysis. Figure 3.12a shows the overview of the results for a touch being analyzed in normal direction. The mean impedance varies between 10 and 20 dB with a resonance in the range

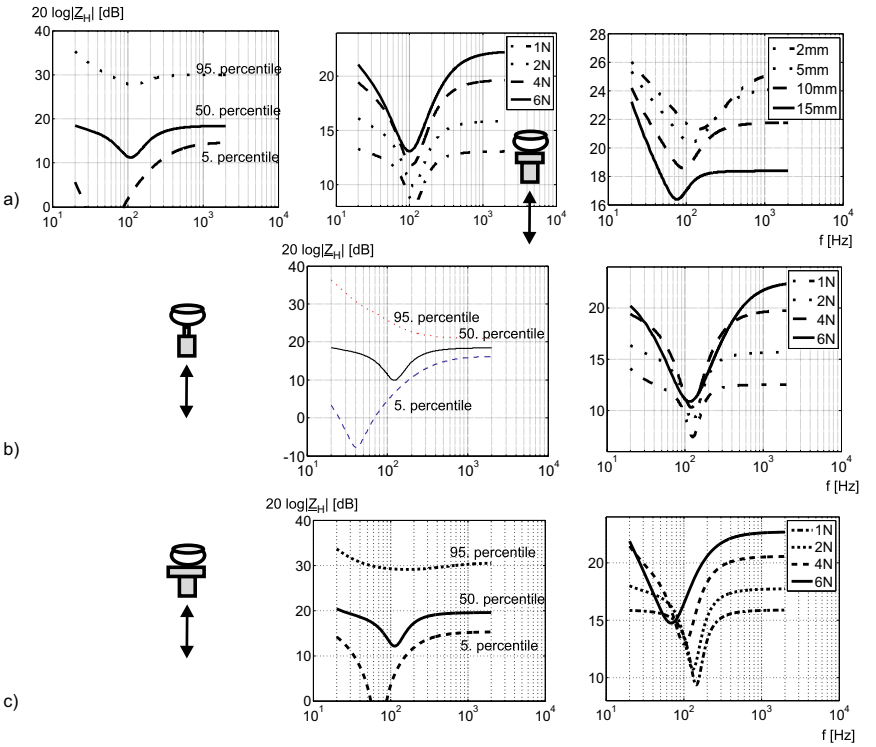

Fig. 3.12 Impedance of finger touch via a cylindrical plate for different contact forces (1–6 N) and in dependency from diameter (**a**), for the smallest plate (Ø 2 mm) and the largest plate (Ø 15 mm) (defined for 20–2 kHz)

of 100 Hz. Throughout all measured diameters of contactor size and forces, no significant dependency of the position of the anti-resonance on touch forces were noted. However, a global increase in impedance is clearly visible. Observing the impedance dependent on contactor size, we can recognize an increase of the anti-resonance frequency. Additionally, it is fascinating to see that the stiffness decreases with an increase of contact area. The increase in resonance is probably a result of less material and therefore less inertia participating in generating the impedance. The increase in stiffness may be a result of smaller pins deforming the skin more deeply and therefore getting nearer to the bone as a stiff mechanical counter bearing.

In comparison, with measurements performed with a single pin of only 2 mm in diameter (Fig. 3.12b), the general characteristic of the force dependency can be reproduced. Looking at the largest contact element of 15 mm, in diameter, we are aware of a movement of the resonance frequency from 150 Hz to lower values down to 80 Hz for an increase in contact force.

In orthogonal direction the skin results differ slightly. Figure 3.13a shows a lateral excitation of the finger pad with an obvious increase of impedance at increased force

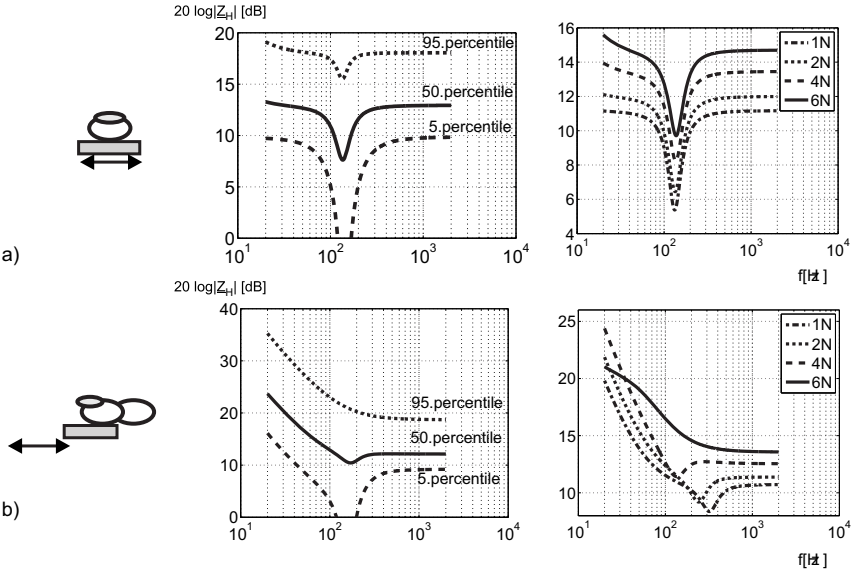

Fig. 3.13 Impedance for finger touch of a plate moving in orthogonal direction to the skin at different force levels (1–6 N) (defined for 20 Hz to 2 kHz). Movement in lateral direction (**a**), distal direction (**b**)

of touch. This rise is mainly a result of an increase of damping parameters and masses. The position of the anti-resonance in frequency domain remains constant at around 150 Hz. The picture changes significantly for the impedance in distal direction (Fig. 3.13b). The impedance still increases, but the resonance moves from high frequencies of around 300 Hz to lower frequencies. Damping increases too, resulting in the anti-resonance being diminished until non-existence.

3.1.6.3 Superordinate Comparison of Grasps

It is interesting to compare the impedances among different types of touch and grasps with each other:

- Almost all raw data and the interpolated models show a decrease of impedance within the lower frequency range of 20 Hz to the maximum of the first anti-resonance. As to precision grasps (Figs. 3.9, 3.10 and 3.11), normal fingertip excitation (Fig. 3.12), the gradient equals 20 dB/decade resembling a dominating pure elongation proportional effect of force response—elasticity—within a low frequency range. Within this low bandwidth-area nonlinear effects of tissue including damping seem to be not very relevant. Looking at this type of interactions we can assume that any interaction including joint rotation of a finger is almost purely elastic in a low frequency range.

- Many models show a clear antiresonance. Its position varies between 200 Hz or even 300 Hz at finger touch analyzed in orthogonal direction (Fig. 3.13). The resonance is a natural effect of any system including a mass and elasticity. Therefore it is not its existence which is relevant for interpretation, but its shape and the position within the frequency range. As to positions, the precision grasps of a cylinder in a pen-like position (Fig. 3.9) and in horizontal position (Fig. 3.11) and the touch of an orthogonal moving plate in distal direction (Fig. 3.13b) and a large plate in normal direction (Fig. 3.13a) have a clear dependence on grasping force. The interpretation is not as obvious as in case one. We assume that the normal touch of the plate shows similarities to the contact situation when touching the rings. Additionally the normal touch is part of the precision grasps mentioned above. In the case of many subjects grasping the horizontal cylinder, it could be observed that the thumb was positioned less orthogonally but more axially to the cylinder, which could excite it primarily in distal direction, thus also contributing to this effect.
- The shape of the anti-resonance is another interesting factor. It can be noted that especially in the analysis of finger grasps and there at orthogonal excitation (Fig. 3.13a), the anti-resonance is very narrow. An interpretation is hard to be formulated. It seems that with grasps and especially touches involving less material the anti-resonance becomes narrower in shape.
- For all measurements, at high frequencies above the anti-resonance, the frequency characteristic becomes linear and constant, which resembles a pure damping effect. This becomes obvious at the pen-hold posture among the precision grasps (Fig. 3.9) and with the lateral displacement in orthogonal direction, (Fig. 3.13a), but is part of any curve and model. Alternatively, inertia could be assumed to dominate the high frequencies, being represented by a linear increase of mechanical impedance. This measured effect is especially relevant, as it confirms common assumptions that for high frequency haptic playback with kinaesthetic devices, the user can be assumed as a damping load.
- A last glance should be taken at the absolute height level and the variance of height of the impedance due to pre-loads. For all grasps it varies in a range (regarding the median curves only) of 20 dB as a maximum. Impedance is higher for power grasps, slightly lower for precision grasps and very much lower for touches, which is immediately obvious. The change in the pre-load for one grasp typically displaces the absolute impedance to higher levels. This displacement varies between 4 and 10 dB.

If speculations should be made on still unknown, not yet analyzed types of touches according to the given data, it should be reasonable to assume the following:

A. **Power grasp** The median impedance should be around 36 dB. Model the impedance with a dominating elasticity effect until an anti-resonance frequency of 80 Hz, not varying much neither in height nor in position of the anti-resonance. Afterward, allow inertia to dominate the model's behavior.
B. **Precision grasp** The median impedance should be around 25 dB. Model the impedance with a dominating elasticity effect until an anti-resonance frequency

of around 200 Hz. The position of the anti-resonance diminishes in an area of 100 Hz due to change in pre-load. Above that anti-resonance let the impedance become dominated by a damping effect. The height of impedance changes in a range of 5 dB by the force of the grasp.

C. **Finger touch** The median impedance should be around 12 dB. Model the impedance with a well balanced elasticity and damping effect until an anti-resonance frequency of around 150 Hz. The position of the anti-resonance is quite constant, with the exception of large contact areas moving in normal and in distal direction. Above that anti-resonance let the impedance become strongly dominated by a damping effect. The absolute height of impedance changes in an area of up to 10 dB depending on the force during touch.

3.1.7 Comparison with Existing Models

For further insight into and qualification of the results, a comparison with published mechanical properties of grasps and touches is presented in this section. There are two independent trends of impedance analysis in the scientific focus: the measurement of mechanical impedance as a side product of psychophysical studies at threshold level, and measurements at higher impedance levels for general haptic interaction. The frequency plots of models and measurements are shown in Fig. 3.14.

In [14] the force detection thresholds for grasping a pen in normal orientation have been analyzed. Figure 3.14a shows an extract of the results compared to the pen-like grasp of a cylinder of the model in Fig. 3.9a. Whereas the general level of

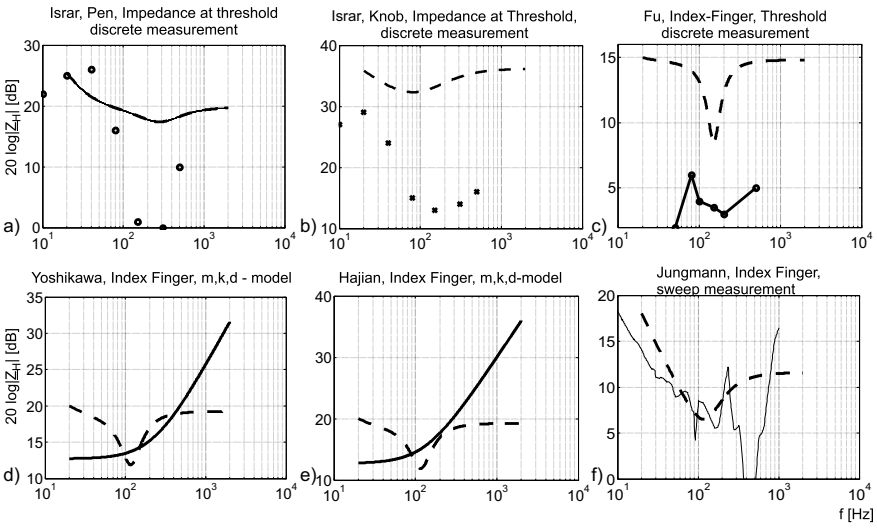

Fig. 3.14 Comparison of the model from Fig. 3.8 with data from similar touches and grasps as published by ISRAR [14, 15], FU [8], YOSHIKAWA [29], HAJIAN [10], JUNGMANN [17]

impedance does fit, the dynamic range covered by our model is not as big as described in literature. Analyzing the data as published, we can state that the minimum force measured by ISRAR is ≈60 μN at the point of lowest impedance. A force sensor reliably measuring at this extreme level of sensitivity exceeds the measurement error of our setup and may be the explanation of the difference in the dynamic range covered. In another study [15] the force detection threshold of grasping a sphere with the finger tips was analyzed. The absolute force level of interaction during these measurements was in the range of mN. A comparison (Fig. 3.14b) between our model of touching a sphere and these data show a difference in the range of 10–20 dB. However such small contact forces resemble a large extrapolation of our model data to low forces. The difference can therefore be easily explained by the error resulting from this extrapolation.

FU [8] measured the impedance of the finger tip at a low force of 0.5 N. He advanced an approach published by HAJIAN [10]. A comparison between our model and their data concerning the shape is hardly possible due to the little number of discrete frequencies of this measurement. However the impedance is again 10 dB lower than of our touch model of a five millimeter cylinder at normal oscillations similar to Fig. 3.12. Once more the literature data describe a level of touch force not covered by our measurements and therefore the diagram in Fig. 3.14c is an extrapolation of the model of these low forces.

As a conclusion of this comparison, the model presented here cannot necessarily be applied to measurements done at lower force levels. Publications dealing with touch and grasp at reasonable interaction forces reach nearer to the model parameter estimated by our research. YOSHIKAWA [29] published a study of a three element mechanical model regarding the index finger. The study was based on a time-domain analysis of a mechanical impact generated by a kinaesthetic haptic device. The measured parameters result in a frequency plot (Fig. 3.14d) which is comparable to our model of low frequencies, but does neither show the complexity nor the variability of our model in a high frequency range of above 100 Hz. A similar study in time-domain was performed by HAJIAN [10] with just slightly different results. Measurements available as raw data from JUNGMANN [17] taken in 2002 come quite close to our results, although obtained with different equipment.

Besides these frequency plots, the model's parameters allow a comparison with absolute values published in literature: SERINA [26] made a study on the hysteresis of the finger tips' elongation vs. force curve during tapping experiments. This study identified a value for k for pulp stiffness ranging from 2 N/mm at a maximum tapping-force of 1–7 N/mm at a tapping force of 4 N. This value is about 3–8 times larger than the dominating k_2 in our eight-element model. The results of FU [8] make us assume that there was a systematic error concerning the measurements of SERINA, as the elongation measured at the fingernail does not exclusively correspond to the deformation of the pulp. Therefore the difference in the values of k between our model and their measurements can become reasonable. Last but not least MILNER [22] carried out several studies on the mechanical properties of the finger tip in different loading directions. In the relevant loading situation a value of k ranging

from 200 to 500 N/m was identified by him. This is almost perfect within the range of our model's stiffness.

3.1.8 Modeling User's Variability

In order to perform an optimal system and control design, a good modeling of user's variability should be included. The key for a good variability modeling is precise measurments. FU ET AL. [7] performed a variability analysis especially for stylus-based haptic devices. The variability of human arm was studied in two forms: structured and unstructured variability. Structured was defined as the statically defined uncertainties from the paramters of the human arm model used. On the other hand the multiplicative unstructured uncertainties we referred as unstructured variability. Both variability forms are modeled in a way, such that they can be applied directly to a robust stability analysis.

3.1.9 Final Remarks on Impedances

The impedance model as presented here will help with the modeling of haptic perception in high frequency ranges of above 20 Hz. However, it completely ignores any mechanical properties below that frequency range. This is a direct consequence of the general approach to human machine interaction presented in Chap. 2 and has to be considered when using this model.

Another aspect to consider is that the above measurements show a large inter-subject variance of impedances. In extreme cases they span 20 dB meaning nothing else but a factor of 10 between e.g. the 5th and the 95th percentile. Further research on the impedance models will minimize this variance and allow a more precise picture of impedances. But already this database, although not yet completed, allows to identify helpful trends for human load and haptic devices.

3.2 The User as a Measure of Quality

Christian Hatzfeld

SALISBURY ET AL. postulated a very valuable hypothesis for the design of task-specific haptic systems: Their 2011 paper title reads *What You Can't Feel Won't Hurt You: Evaluating Haptic Hardware Using a Haptic Contrast Sensitivity Function* [25]. In this work, they use haptic contrast sensitivity functions (the inverse of the sinusoidal grating detection threshold) to evaluate ↪ COTS devices. With a more general view, the first part of this paper title summarizes the second role of the user and

her or his properties in the design of haptic systems: As the instance that determines, whether the presented haptic feedback is good enough or not. In this section, this approach is detailed on three aspects of the system design, i.e. resolutions, errors and the quality of the haptic interaction.

3.2.1 Resolution of Haptic Systems

Resolution is mainly an issue in the selection and design of sensors and actuators, while latter is also influenced by the kinematic structure used in interfaces and manipulators. In general, sensors on the manipulation side have so sense at least as good as the human user is able to perceive after the information is haptically displayed by the haptic interface. On the interface side, sensors have to be at least as accurate as the reproducibility of the human motor capability, to convey the users intention correctly. For the actuating part, the attribution is vice versa: actuators on the manipulating side have to be as accurate as the human motor capability, while the haptic interface has to be as accurate as human perception can resolve.

Unfortunately, this is the worst case for technical development: sensors (on the manipulating side) and actuators (on the interfacing side) have to be as accurate as human perception. Therefore exact readings of *absolute thresholds* are indispensable to determine the necessary resolutions for sensors and actuators, if one wants to build a high-fidelity haptic system. On the other hand, systematic provisions to alter the perception thresholds favourably by changing the contact situation (contact area, contact forces) at the primary interface are possible. This is further detailed in Sect. 5.2.

For applications not involving teleoperation, the requirements are basically the same, but extend to other parts of the system: For the interaction with virtual realities, the software has to supply sufficient discretization of the virtual data (a non-trivial problem, especially if small movements and hard contacts are to be simulated), systems for communication have to supply enough mechanical energy that the perception threshold is surpassed to ensure clear transmission of information. Last, but definitely not least, all errors resulting from digital quantization and other, system inherent noise have to be lower than the absolute perception thresholds of the human user.

3.2.2 Errors and Reproducibility

While resolutions are quite a challenge for the design of haptic systems because of the high sensitivity of human haptic perception, the handling of errors is somewhat easier. The basic assumption about the perception of haptic signals with regard to errors and reproducibility is the following: There is no error, if there is no difference detectable by the user. This property is expressed by the ↪ JND. *Weber's Law* as

stated in Eq. (2.5) facilitates this further: For low references the acceptable error increases due to the increasing differential thresholds. This accommodates the fact, that the absolute errors of technical systems and components usually increase, when the reference values decrease.

For large reference values, this relative resolution of human perception is much smaller than the absolute resolution of technical systems, that is uniformly distributed along the whole nominal range. This has to be taken into account if information are to be conveyed haptically.

3.2.3 Quality of Haptic Interaction

While resolution and errors are pretty much linked directly to perception parameters, the assessment of haptic quality is somewhat more difficult. It is also based on the assumption, that the quality of a haptic interaction is good enough, if all intended information are transmitted correctly to the user and no additional information or errors are perceived. The second part can basically be achieved by considering the above mentioned points regarding errors and resolution. The assessment, if all information is transmitted correctly is more difficult, since the user and the perceived information have to be taken into account. In general, this is only possible if suitable evaluation methods are used, Chap. 13 gives an overview about such methods with respect to the intended application.

Another example for the evaluation of haptic quality is the concept of haptic transparency for teleoperation system. This property describes the ability of a haptic system to convey only the intended information (normally defined as the mechanical impedance of the environment at the manipulator side $\underline{Z}_e$) to the user (in terms of the displayed impedance of the haptic interface $\underline{Z}_t$) without displaying the inherent properties of the haptic system. This definition is further detailed in Sect. 7.5.2. Despite the above said, this property can be tested without a user test, but with considerable effort regarding the mechanical measurement setup.

When further considering haptic perception properties, especially ↪ Just Noticeable Differences, the common binary definition of transparency can be transformed to a nominal value with a lot less requirements on the technical system. This concept was developed by HATZFELD ET AL. [12, 13] and is further explained in Sect. 7.5.2.

One should keep in mind, that all of the above mentioned thresholds are generally dependent on frequency and the contact situation in the best case. In the worst case, they are also dependent on the experimental methodology used to obtain them, which will necessarily require a retest of the perception property needed.

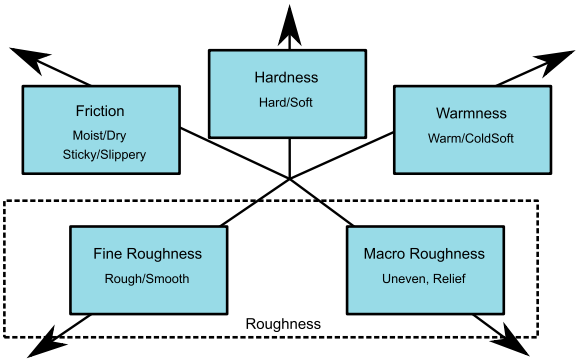

Fig. 3.15 Five psychophysical dimensions of tactile perception for materials and textures, based on OKAMOTO ET AL. [24]

3.2.4 Perceptional Dimensions

All above approaches follow the tendency to describe quality of haptic interaction by perceptional capabilities in a usually physical domain. The inherent assumption is that humans act as sensors for physical properties. Stating this in an explicit way makes it obvious that this can not be true.

This is where *perceptional dimensions* should be considered. All psychophysical fields use this more user-centric approach. And the range for *perceptional dimensions* is wide, from object perception to space perception as nicely summarized by KAPPERS AND BERGMANN TIEST in [19].

However the level of difference between physical and perceptional dimensions is nowhere larger than in the domain of *textures*. OKAMOTO ET AL. identified in a review [24] five dominating tactile dimensions for textures (Fig. 3.15). This triggered systematic research on the discrimination of materials (e.g. [4]) and new quality measures for performance evaluations of texture-rendering devices (e.g. [27]).

Recommended Background Reading

[16] Jones, L. & Lederman, S.: **Human Hand Function**. Oxford University Press, 2006
Extensive Analysis about the human hand including perception and interaction topics.

[6] Feix, T.; Pawlik, R.; Schmiedmayer, H.; Romero, J. & Kragic, D.: **A Comprehensive Grasp Taxonomy** In: Robotics, Science and Systems Conference: Workshop on Understanding the Human Hand for Advancing Robotic Manipulation, 2009.
Thorough Analysis of human grasps, also available online at http://grasp.xief.net/.

References

1. Bochereau S et al (2017) Characterizing and imaging gross and real finger contacts under dynamic loading. IEEE Trans Hapt 10(4):456–465
2. Brownjohn J et al (1980) Errors in mechanical impedance data obtained with impedance heads. J Sound Vibr 73(3):461–468. https://doi.org/10.1016/0022-460X(80)90527-1
3. Bullinger H-J (1978) Einflußfaktoren und Vorgehensweise bei der ergonomischen Arbeitsmittelgestaltung. Universität Stuttgart, Habilitation
4. Culbertson H, Kuchenbecker KJ (2017) Importance of matching physical friction, hardness, and texture in creating realistic haptic virtual surfaces IEEE Trans Hapt 10(1):63–74. ISSN: 19391412. https://doi.org/10.1109/TOH.2016.2598751
5. Feix T (2012) Human grasping database. Letzter Abruf: 20 Mar 2012. http://grasp.xief.net
6. Feix T et al (2009) A comprehensive grasp taxonomy. In: Robotics, science and systems conference: workshop on understanding the human hand for advancing robotic manipulation. http://grasp.xief.net/documents/abstract.pdf
7. Fu MJ, Cavusoglu MC (2012) Human-arm-and-hand-dynamic model with variability analyses for a stylus-based haptic interface. IEEE Trans Syst Man Cybern Part B: Cybern 42(6):1633–1644. ISSN: 10834419. https://doi.org/10.1109/TSMCB.2012.2197387
8. Fu C-Y, Oliver M (2005) Direct measurement of index finger mechanical impedance at low force. In: Eurohaptics conference, 2005 and symposium on haptic interfaces for virtual environment and teleoperator systems. World haptics 2005. First Joint Embedded System & Physical Sciences Research Laboratory, Motorola Labs, USA, pp 657–659. https://doi.org/10.1109/WHC.2005.40
9. Fung Y-C (1993) Biomechanics: mechanical properties of living tissues. 2nd edn. New York [u.a.]: Springer. pp XVIII, 568. ISBN: 0-387-97947-6; 3-540-97947-6
10. Hajian AZ, Howe RD (1997) Identification of the mechanical impedance at the human finger tip. J Biomech Eng 119:109–114. https://doi.org/10.1115/1.2796052
11. Hannaford B, Anderson R (1988) Experimental and simulation studies of hard contact in force reflecting teleoperation. In: Proceedings IEEE International Conference on Robotics & Automation. Jet Propulsion Laboratory, Caltech, Pasadena, CA, USA, pp 584–589. https://doi.org/10.1109/ROBOT.1988.12114
12. Hatzfeld C (2013) Experimentelle Analyse der menschlichen Kraftwahrnehmung als ingenieurtechnische Entwurfsgrundlage für haptische Systeme. Dissertation, Technische Universität Darmstadt. München: Dr. Hut Verlag. http://tuprints.ulb.tu-darmstadt.de/3392/. ISBN: 978-3-8439-1033-0
13. Hatzfeld C, Neupert C, Werthschützky R (2013) Systematic consideration of haptic perception in the design of task-specific haptic systems. Biomed Tech 58. https://doi.org/10.1515/bmt-2013-4227
14. Israr A, Choi S, Tan HZ (2006) Detection threshold and mechanical impedance of the hand in a pen-hold posture. In: International conference on intelligent robots and systems (IROS), Peking, C, pp 472–477. https://doi.org/10.1109/IROS.2006.282353
15. Israr A, Choi S, Tan HZ (2007) Mechanical impedance of the hand holding a spherical tool at threshold and suprathreshold stimulation levels. In: Second joint eurohaptics conference and symposium on haptic interfaces for virtual enrivonment and teleoperator systems (WorldHaptics conference), Tsukaba. https://doi.org/10.1109/WHC.2007.81
16. Jones L, Lederman S (2006) Human hand function. Oxford University Press, Oxford, GB. 0195173155
17. Jungmann M, Schlaak HF (2002) Taktiles Display mit elektrostatischen Polymeraktoren. In: Konferenzband des 47. Internationalen Wissenschaftlichen Kolloquiums, Technische Universität Ilmenau. http://tubiblio.ulb.tu-darmstadt.de/17485/
18. Jungmann M (2004) Entwicklung elektrostatischer Festkörperaktoren mit elastischen Dielektrika für den Einsatz in taktilen Anzeigefeldern. Dissertation. Technische Universität Darmstadt, p 138. http://tuprints.ulb.tu-darmstadt.de/500/

19. Kappers AM, Bergmann Tiest WM (2013) Haptic perception. Wiley Interdisc Rev: Cogn Sci 4(4):357–374. https://doi.org/10.1002/wcs.1238
20. Kern T et al (2006) Study of the influence of varying diameter and grasp-forces on mechanical impedance for the grasp of cylindrical objects. In: Proceedings of the Eurohaptics conference, Paris, F. https://doi.org/10.1007/978-3-540-69057-3_21
21. Kunstmann C (1999) Handhabungssystem mit optimierter Mensch-Maschine-Schnittstelle für die Mikromontage. VDI-Verlag, Düsseldorf. 978-3-642-57024-7
22. Milner TE, Franklin DW (1998) Characterization of Multijoint finger stiffness: dependence on finger posture and force direction. IEEE Trans Biomed Eng 43(11): Diss, 1363–1375. https://doi.org/10.1109/10.725333
23. Oguztoreli MN, Stein RB (1990) Optimal task performance of antagonistic muscles. Biol Cybern 64(2):87–94. https://doi.org/10.1007/BF02331337
24. Okamoto S, Nagano H, Yamada Y (2013) Psychophysical dimensions of tactile perception of textures. IEEE Trans Hapt 6(1):81–93. ISSN: 19391412. https://doi.org/10.1109/TOH.2012.32
25. Salisbury C et al (2011) What you can't feel won't hurt you: evaluating haptic hardware using a haptic contrast sensitivity function. IEEE Trans Hapt 4(2):134–146. https://doi.org/10.1109/TOH.2011.5
26. Serina Elaine R, Mote C, Rempel D (1997) Force response of the fingertip pulp to repeated compression—effects of loading rate, loading angle and anthropometry. J Biomech 30(10):1035–1040. https://doi.org/10.1016/S0021-9290(97)00065-1
27. Strohmeier P, Hornbaek K (2017) Generating haptic textures with a vibrotactile actuator. In: Proceedings of the 2017 CHI conference on human factors in computing systems proceeding, pp 4994–5005. https://doi.org/10.1145/3025453, http://dx.doi.org/10.1145/3025453.3025812
28. Wiertlewski M, Hayward V (2012) Mechanical behavior of the fingertip in the range of frequencies and displacements relevant to touch. J Biomech 45(11):1869–1874. https://doi.org/10.1016/j.jbiomech.2012.05.045
29. Yoshikawa T, Ichinoo Y (2003) Impedance identification of human fingers using virtual task environment. In: Proceedings 2003 IEEE/RSJ International Conference on Intelligent Robots and Systems (IROS 2003), vol 3, pp 3094–3099. https://doi.org/10.1109/IROS.2003.1249632